arXiv:1407.5717v2 [cond-mat.mes-hall] 3 Nov 2014

Electrical transport through a quantum dot side-coupled to a topological superconductor

Yu-Li Lee*
Department of Physics, National Changhua University of Education, Changhua, Taiwan, Republic of China
(Dated: November 4, 2014)

We propose to measure the differential conductance G as a function of the bias V for a quantum dot side-coupled to a topological superconductor to detect the existence of the chiral Majorana edge states. It turns out that G for the spinless dot is an oscillatory (but not periodic) function of eV due to the coupling to the chiral Majorana edge states, where $-e$ is the charge carried by the electron. The behavior of G versus eV is distinguished from the one for a multi-level dot in three respects. First of all, due to the coupling to the topological superconductor, the value of G will shift upon adding or removing a vortex in the topological superconductor. Next, for an off-resonance dot, the conductance peak in the present case takes a universal value $e^2/(2h)$ when the two leads are symmetrically coupled to the dot. Finally, for a symmetric setup and an on-resonance dot, the conductance peak will approach the same universal value $e^2/(2h)$ at large bias.

PACS numbers: 73.63.-b 73.21.-b 74.45.+c

I. INTRODUCTION

Recently, to search for the topological phases and to study their properties become crucial issues in condensed matter physics. Among these topological matters, Majorana fermions, which were theoretically predicted to exist at the edge or the core of a vortex in a $p_x + ip_y$-wave superconductor and superfluid,[1–3] attract a lot of attentions. This is largely triggered by the fact that Majorana fermions are stable against local perturbations[4] and obey the non-Abelian statistics,[5] so that they have great potential in the applications of fault-tolerant quantum computations.[6,7]

Up to now, there are two main theoretical proposals to realize Majorana fermions. One way is to generate a localized Majorana mode at the end of a spin-orbit coupled nanowire subjected to a magnetic field and proximate to an s-wave superconductor,[8,9] which is motivated by a model proposed by Kitaev.[4] Experimental evidence for such a Majorana edge mode was obtained in indium antimonide quantum wires.[10,11] Majorana fermions can also be supported in the vortices of s-wave superconductors deposited on the surface of a three-dimensional topological insulator.[12] In particular, chiral Majorana edge states can be created at the interface between a superconductor and the area gapped by ferromagnetic materials.[12]

One of the challenges in the physics of Majorana fermions is to detect and to verify the existence of Majorana fermions. Several methods have been proposed, including the noise measurement,[13,14] resonant Andreev reflection,[15] and the 4π-periodic Josephson effect.[8,9,16–18] Recently, several groups proposed to measure the electric transport through a quantum dot (QD) coupled to the end of a one-dimensional (1D) topological superconductor (TSC) to detect the existence of Majorana modes[19–21] as well as their dynamics.[22] Especially, in the case of a spinless QD side-coupled to the end of a TSC, the zero-bias conductance at zero temperature takes the value $e^2/(2h)$,[20,21] instead of e^2/h. This fact has been identified as the evidence of the existence of Majorana end modes. In the present work, we propose to employ the similar idea to detect the chiral Majorana edge states in the TSC.

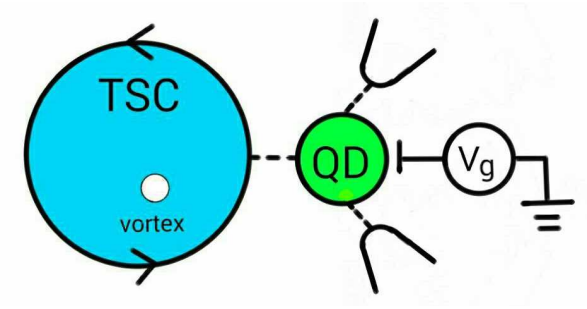

FIG. 1: (Color online) A schematic setup of a QD side-coupled to a TSC and to two metallic leads. The dot level can be controlled by a capacitively coupled gate voltage V_g. The bias is applied between two leads. The TSC is formed by depositing a superconducting island on a three-dimensional topological insulator. The area outside the superconductor is gapped by ferromagnetic materials. At the interface between the superconductor and the ferromagnetic material, there is a branch of chiral Majorana fermions denoted by the arrow.

A schematic setup is shown in Fig. 1. The QD, which can be formed by using either graphene[23] or the carbon nanotube,[24] is side-coupled to a TSC and to two metallic leads. The dot level can be controlled by a capacitively coupled gate voltage V_g. The bias V is applied between two leads. The TSC is formed by depositing a superconducting island on a three-dimensional (3D) topological insulator. (The possible candidates of 3D topological insulators are Bi_2Se_3 or Bi_2Te_3.[25]) The area outside the superconductor is gapped by ferromagnetic materials. At the interface between the superconductor and the ferromagnetic material, there is a branch of chiral Majorana fermions. The presence of the ferromagnetic material re-

moves spin degeneracy of the dot levels. Suppose that the Zeeman splitting is large enough. We may assume that the dot electrons are spinless.[26] For such a case, we found that the differential conductance G through the spinless dot is an oscillatory (but not periodic) function of eV due to the coupling to the chiral Majorana edge states, where $-e$ is the charge carried by the electron. The behavior of G versus eV in the present case is distinguished from the one for a multi-level dot in three respects. First of all, the value of G for the former will shift upon adding or removing a vortex in the TSC. Next, for an off-resonance dot, the conductance peak for the former takes a universal value $e^2/(2h)$ when the two leads are symmetrically coupled to the dot. Finally, for a symmetric setup and an on-resonance dot, the conductance peak in the present case will approach the same universal value $e^2/(2h)$ at large bias.

The rest of the paper is organized as follows. We first write down the Hamiltonian which models the setup in Fig. 1 and discuss the approximations we made in the calculations. Next, we present the relevant Green functions to calculate the current through the dot. Then, we give the spectral function of the dot electrons, the differential conductance, and the relevant stuffs. The final section is devoted to a summary of our results.

II. THE MODEL

We consider a setup shown in Fig. 1. The TSC is realized by depositing a superconducting island on the surface of a three-dimensional topological insulator. The region outside the superconductor is gapped by ferromagnetic materials. This system can be modeled by the Hamiltonian: $H = H_C + H_D + H_T$, where

$$H_C = \sum_{\alpha\in L,R}\sum_{\boldsymbol{k}} \epsilon_{\boldsymbol{k}\alpha} c^\dagger_{\boldsymbol{k}\alpha} c_{\boldsymbol{k}\alpha} \ , \tag{1}$$

describes the leads, and

$$H_T = \sum_{\alpha\in L,R}\sum_{\boldsymbol{k}} \frac{V_{\boldsymbol{k}\alpha}}{\sqrt{\Omega}} c^\dagger_{\boldsymbol{k}\alpha} d + \text{H.c.} \ , \tag{2}$$

describes the tunneling between the leads and the dot. The presence of the ferromagnetic material will split the electronic levels of the dot with different spins. We shall focus on the case with large Zeeman splitting such that within the energy scale in which we are interested the dot electrons can be regarded as spinless fermions. We further assume that eV and k_BT are much smaller than the superconducting gap in the TSC and the average level spacing in the dot, where T is the temperature. Within these approximations, the Hamiltonian H_D can be written as

$$H_D = \epsilon_d d^\dagger d + \frac{v_M}{2}\int_{-L/2}^{L/2} dx \eta(-i\partial_x\eta) - i\bar{t}\eta(0)(\xi d + \text{H.c.}) \ , \tag{3}$$

where $\bar{t} > 0$ denotes the tunneling amplitude between the dot and the Majorana edge states, ξ is a complex number with $|\xi| = 1$, $|v_M|$ is the speed of Majorana fermions, and L is the circumference of the island. In Eq. (3), we have taken $x = 0$ as the contact point between the TSC and the dot. The dot level ϵ_d can be adjusted by a capacitively coupled gate voltage V_g.

The real field $\eta(x)$, which describes the chiral Majorana edge states, obeys the anticommutation relation

$$\{\eta(x), \eta(y)\} = \delta(x-y) \ .$$

The Fourier decomposition of $\eta(x)$ is given by

$$\eta(x) = \frac{1}{\sqrt{L}}\sum_k \psi_k e^{ikx} \ ,$$

where ψ_k and $\psi_k^\dagger$ obey the canonical anticommutation relations. Since η is a real field, we have $\psi_{-k} = \psi_k^\dagger$. The boundary condition of $\eta(x)$ depends on the number of vortices N_v in the TSC:

$$\eta(L/2) = (-1)^{N_v+1}\eta(-L/2) \ ,$$

which leads to $k = \frac{(2n+N_v+1)\pi}{L}$ with $n = 0, \pm1, \pm2, \cdots$.

For simplicity, we assume that $V_{\boldsymbol{k}\alpha}$ is independent of $\boldsymbol{k}$, leading to the level-width functions $\Gamma_{L(R)}(E) = 2\pi|V_{L(R)}|^2 N_{L(R)}(E)$, where $N_{L(R)}(E)$ is the density of states for electrons in the left (right) lead. We further ignore the energy dependence of $\Gamma_{L(R)}(E)$. Within these approximations, the current can be calculated by a Landauer-type formula:[27]

$$I = -\frac{e\Gamma_L\Gamma_R}{2\pi\Gamma}\int_{-\infty}^{+\infty} dE[f_L(E) - f_R(E)]A(E) \ , \tag{4}$$

where $\Gamma = \Gamma_L + \Gamma_R$ and $f_{L(R)}(E) = [e^{\beta(E-\mu_L)} + 1]^{-1}$ is the distribution function of electrons in the left (right) lead with $\mu_{L(R)}$ being the corresponding chemical potential and $\beta = (k_BT)^{-1}$. We shall take $\mu_L - \mu_R = -eV$. Moreover, we set $\mu_L = 0 = \mu_R$ in equilibrium. In Eq. (4), $A(E) = -2\text{Im}[D_r(E)]$ is the spectral function for dot electrons and $D_r(E)$ is the Fourier transform of the retarded Green function for dot electrons:

$$D_r(t_1, t_1) = -i\Theta(t_1 - t_2)\langle\{d(t_1), d^\dagger(t_2)\}\rangle \ .$$

By taking $\mu_L = -eV/2$ and $\mu_R = eV/2$, we find that

$$G(V) = \frac{dI}{dV} = \frac{\Gamma_L\Gamma_R}{\Gamma}\left[\frac{A(eV/2) + A(-eV/2)}{2}\right]G_0 \ , \tag{5}$$

at $T = 0$, where $G_0 = e^2/(2\pi)$ is the conductance quantum for spinless electrons. Equation (5) indicates that $G(V)$ measures the symmetric part of $A(E)$. Hence, the rest of the task is to calculate $A(E)$.

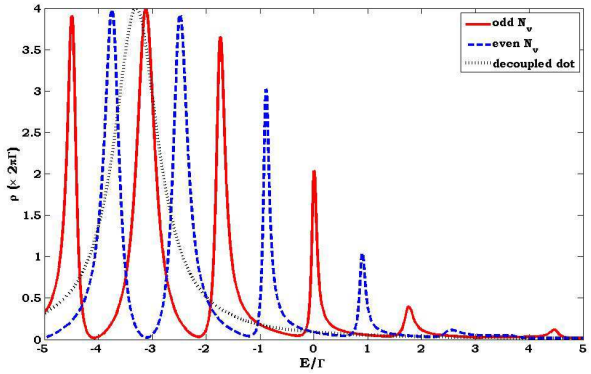

FIG. 2: (Color online) LDOS's for the dot. Solid (dashed) line represents the case with an odd (even) number of vortices in the superconductor. We take $\Gamma_L = \Gamma_R = \Gamma/2 = 0.5\pi v_M/L$, $\epsilon_d = -3.3\Gamma$, and $\bar{t}^2/v_M = 2\Gamma$. The location of the peak will shift when a vortex is added or removed. For comparison, the dotted line corresponds to the case with $\bar{t} = 0$.

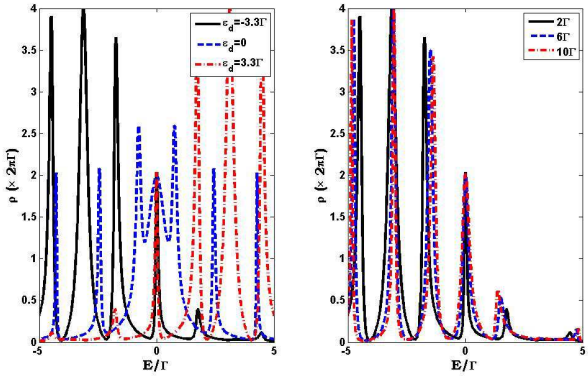

FIG. 3: (Color online) LDOS's for the dot with odd N_v. We take $\Gamma_L = \Gamma_R = \Gamma/2 = 0.5\pi v_M/L$. **Left**: $\rho(E)$ with $\bar{t}^2/v_M = 2\Gamma$ for different values of ϵ_d. The location of the resonance depends on the value of ϵ_d sensitively. **Right**: $\rho(E)$ with $\epsilon_d = -3.3\Gamma$ for different values of $\bar{t}^2/v_M$. The location of the resonance also slightly depends on the value of $\bar{t}^2/v_M$.

III. ELECTRICAL TRANSPORT THROUGH A SPINLESS DOT

A. The local density of states for dot electrons

One way to calculate $D_r(E)$ is to employ the method of equations of motion (EOM). Within the approximation we have made, the set of EOM's for two-point Green functions is closed and one may get an exact form of $D_r(E)$:

$$D_r(E) = \frac{E + \epsilon_d - M(E) + \frac{i}{2}\Gamma}{\left[E - M(E) + \frac{i}{2}\Gamma\right]^2 - \epsilon_d^2 - [M(E)]^2}\ , \qquad (6)$$

where

$$M(E) = -\frac{\bar{t}^2}{2v_M}\tan\left(\frac{L}{2v_M}E - \frac{N_v\pi}{2}\right),$$

arises from the propagator of Majorana fermions. In terms of Eq. (6), the spectral function of the dot electrons takes the form

$$A(E) = \frac{\Gamma\{[E + \epsilon_d - M(E)]^2 + [M(E)]^2 + \frac{\Gamma^2}{4}\}}{\left[E^2 - 2EM(E) - \epsilon_d^2 + \frac{\Gamma^2}{4}\right]^2 + \Gamma^2\{\epsilon_d^2 + [M(E)]^2\}}. \qquad (7)$$

The behavior of the local density of states (LDOS) of the dot, $\rho(E) = A(E)/(2\pi)$, is shown in Figs. 2 and 3.

A few remarks about $\rho(E)$ are in order. First of all, we notice that $\rho(-E, \epsilon_d) = \rho(E, -\epsilon_d)$. Consequently, $\rho(-E) = \rho(E)$ when $\epsilon_d = 0$, as shown in the left diagram in Fig. 3. Next, $\rho(E)$ (or $A(E)$) is an oscillator function of E on account of the coupling to the quantized energy levels of the chiral Majorana edge states. The location of the peak indicates the occurrence of a resonance, which depends on the number of vortices N_v as well as the value of ϵ_d. Variation of the value of $\bar{t}^2/v_M$ also slightly shifts the position of the resonance, but does not change the global feature significantly. For $\epsilon_d < 0$ ($\epsilon_d > 0$), most resonances have energies $E < 0$ ($E > 0$). Especially, a zero-energy resonance always exists when N_v is odd, irrespective of the values of ϵ_d and $\bar{t}^2/v_M$. On the other hand, for an off-resonance dot, there is at least a resonance lying between ϵ_d and 0 when N_v is even.

B. The differential conductance

Inserting Eq. (7) into Eq. (5), we obtain the differential conductance at zero temperature. The behavior of G versus eV is shown in Figs. 4 – 6. We see that G depends on N_v. When N_v is odd, a zero Majorana edge mode exists, which results in a zero-bias peak with the value $G/G_0 = 2\Gamma_L\Gamma_R/\Gamma^2$, even for an off-resonance dot. As noticed in the previous work on the topological superconducting nanowire,[20,21] this is an indication of the existence of a zero-energy Majorana edge mode. For even N_v such that no zero-energy edge modes exist in the TSC, the zero-bias conductance reaches the unitary value $G/G_0 = 4\Gamma_L\Gamma_R/\Gamma^2$ for an on-resonance dot. For an off-resonance dot, the conductance exhibits an oscillatory behavior as varying eV, and reaches half of the value in the unitary limit at the peak. Moreover, there is at least a conductance peak occurring at a value of eV smaller than $2|\epsilon_d|$. These provide evidences for the coupling to quantized energy levels of chiral Majorana edge states. The positions of the conductance peaks shift by varying the gate voltage V_g, but are insensitive to the value of $\bar{t}^2/v_M$. For an on-resonance dot, i.e. $\epsilon_d = 0$, a conductance peak with the value larger than $G/G_0 = 2\Gamma_L\Gamma_R/\Gamma^2$ occurs at a finite bias due to the enhanced side peaks in $\rho(E)$ (or $A(E)$) with odd N_v, as shown in the left diagram in Fig. 3. To sum up, the whole behavior of G with

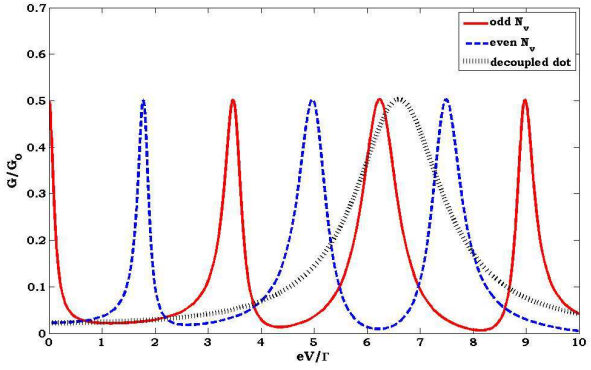

FIG. 4: (Color online) The conductance (in units of G_0) versus eV (in units of Γ). Solid (dashed) line represents the case with an odd (even) number of vortices in the superconductor. We take $\Gamma_L = \Gamma_R = \Gamma/2 = 0.5\pi v_M/L$, $\epsilon_d = -3.3\Gamma$, and $\bar{t}^2/v_M = 2\Gamma$. For comparison, the dotted line corresponds to the case with $\bar{t} = 0$.

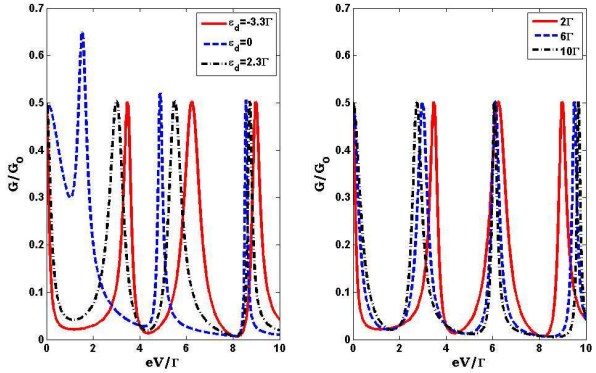

FIG. 5: (Color online) The conductance (in units of G_0) versus eV (in units of Γ) with odd N_v. We take $\Gamma_L = \Gamma_R = \Gamma/2 = 0.5\pi v_M/L$. **Left**: G as a function of eV with $\bar{t}^2/v_M = 2\Gamma$ for different values of ϵ_d. **Right**: G as a function of eV with $\epsilon_d = -3.3\Gamma$ for different values of $\bar{t}^2/v_M$.

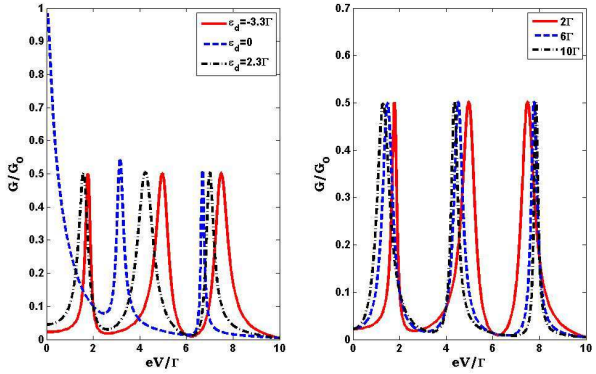

FIG. 6: (Color online) The conductance (in units of G_0) versus eV (in units of Γ) with even N_v. We take $\Gamma_L = \Gamma_R = \Gamma/2 = 0.5\pi v_M/L$. **Left**: G as a function of eV with $\bar{t}^2/v_M = 2\Gamma$ for different values of ϵ_d. **Right**: G as a function of eV with $\epsilon_d = -3.3\Gamma$ for different values of $\bar{t}^2/v_M$.

varying N_v and eV as we have discussed is an indication of the existence of a chiral Majorana liquid at the edge of a TSC.

One may wonder how to distinguish the behavior of G versus eV for a dot side-coupled to a TSC from that for a multi-level dot. According to the above results, both are different in three respects. First of all, the conductance for a dot side-coupled to a TSC will shift upon adding or removing a vortex in the TSC, while the one for a dot decoupled to the TSC remains intact. Next, for an off-resonance dot, the value of the conductance peak in the present case is only half of the one in the unitary limit, whereas for a dot decoupled to the TSC, it will reach a non-universal value depending on the energy levels in the dot as long as $eV/2$ matches one level in the dot. Finally, for an on-resonance dot, the conductance peak in the present case will approach a universal value $G/G_0 = 2\Gamma_L\Gamma_R/\Gamma^2$ at large bias. In general, there is no such a behavior for a dot decoupled to the TSC.

C. The Majorana-fermion representation

The above results can be understood by introducing the Majorana-fermion representation for the dot electrons:

$$\gamma_1 = \frac{\xi d + \xi^* d^\dagger}{\sqrt{2}} \ , \quad \gamma_2 = \frac{\xi d - \xi^* d^\dagger}{\sqrt{2} i} \ ,$$

where γ_i satisfy the anticommutation relation

$$\{\gamma_i, \gamma_j\} = \delta_{ij} \ ,$$

for $i, j = 1, 2$. We notice that only γ_1 couples to the chiral Majorana edge states directly. γ_2 couples the chiral Majorana edge states indirectly through the ϵ_d term, which represents the hopping between γ_1 and γ_2. The retarded Green functions for γ_i, which are defined as

$$iS_j^r(t_1, t_2) \equiv \Theta(t_1 - t_2)\langle\{\gamma_j(t_1), \gamma_j(t_2)\}\rangle \ ,$$

are related to the two-point Green functions of the dot electrons through the following relations:

$$\begin{aligned} S_1^r(t_1, t_2) &= \frac{1}{2}[D_r(t_1, t_2) - D_a(t_2, t_1)] \\ &\quad + \frac{1}{2}\Big[\xi^2 F_r(t_1, t_2) + (\xi^*)^2 \tilde{F}_r(t_1, t_2)\Big] \ , \\ S_2^r(t_1, t_2) &= \frac{1}{2}[D_r(t_1, t_2) - D_a(t_2, t_1)] \\ &\quad - \frac{1}{2}\Big[\xi^2 F_r(t_1, t_2) + (\xi^*)^2 \tilde{F}_r(t_1, t_2)\Big] \ , \end{aligned}$$

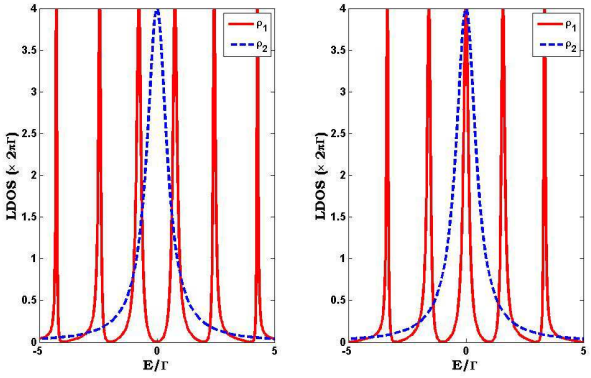

FIG. 7: (Color online) LDOS's for γ_1 and γ_2 with $\epsilon_d = 0$. We take $\Gamma_L = \Gamma_R = \Gamma/2 = 0.5\pi v_M/L$ and $\bar{t}^2/v_M = 2\Gamma$. **Left**: odd N_v. **Right**: even N_v.

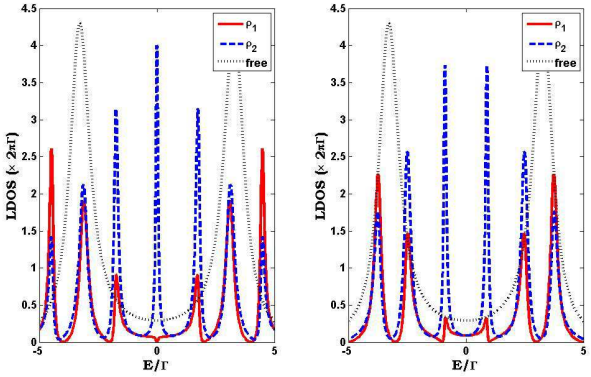

FIG. 8: (Color online) LDOS's for γ_1 and γ_2 with $\epsilon_d = -3.3\Gamma$. We take $\Gamma_L = \Gamma_R = \Gamma/2 = 0.5\pi v_M/L$ and $\bar{t}^2/v_M = 2\Gamma$. **Left**: odd N_v. **Right**: even N_v. For comparison, the dotted line corresponds to the case with $\bar{t} = 0$.

where

$$
\begin{aligned}
iF_r(t,t') &\equiv \Theta(t-t')\langle\{d(t), d(t')\}\rangle \ , \\
i\tilde{F}_r(t,t') &\equiv \Theta(t-t')\langle\{d^\dagger(t), d^\dagger(t')\}\rangle \ ,
\end{aligned}
$$

are anomalous Green functions for dot electrons. By taking the Fourier transform, we get

$$
\begin{aligned}
S_1^r(\omega) &= \frac{1}{2}\Big[D_r(\omega) - D_a(-\omega) + \xi^2 F_r(\omega) + (\xi^*)^2\tilde{F}_r(\omega)\Big] \ , \\
S_2^r(\omega) &= \frac{1}{2}\Big[D_r(\omega) - D_a(-\omega) - \xi^2 F_r(\omega) - (\xi^*)^2\tilde{F}_r(\omega)\Big] \ . \qquad (8)
\end{aligned}
$$

From Eq. (8), we find that

$$
\frac{1}{2}[A(E) + A(-E)] = \pi[\rho_1(E) + \rho_2(E)] \ , \qquad (9)
$$

where $\rho_i(E) = -\frac{1}{\pi}\mathrm{Im}[S_i^r(E)]$ with $i = 1, 2$ are the LDOS's for γ_1 and γ_2. That is, $G(V)$, in fact, measures the sum of the LDOS's for γ_i.

The anomalous Green functions for dot fermions can also be obtained by the method of EOM, yielding

$$
\begin{aligned}
F_r(\omega) &= \frac{(\xi^*)^2 M(\omega)}{\left[\omega - M(\omega) + \frac{i}{2}\Gamma\right]^2 - \epsilon_d^2 - [M(\omega)]^2} \ , \\
\tilde{F}_r(\omega) &= \frac{\xi^2 M(\omega)}{\left[\omega - M(\omega) + \frac{i}{2}\Gamma\right]^2 - \epsilon_d^2 - [M(\omega)]^2} \ . \qquad (10)
\end{aligned}
$$

Inserting Eqs. (6) and (10) into Eq. (8) gives

$$
\begin{aligned}
S_1^r(\omega) &= \frac{\omega + \frac{i}{2}\Gamma}{\left[\omega - M(\omega) + \frac{i}{2}\Gamma\right]^2 - \epsilon_d^2 - [M(\omega)]^2} \ , \\
S_2^r(\omega) &= \frac{\omega - 2M(\omega) + \frac{i}{2}\Gamma}{\left[\omega - M(\omega) + \frac{i}{2}\Gamma\right]^2 - \epsilon_d^2 - [M(\omega)]^2} \ . \qquad (11)
\end{aligned}
$$

Hence, the LDOS's for γ_1 and γ_2 take the forms:

$$
\begin{aligned}
\rho_1(E) &= \frac{\Gamma\left(E^2 + \epsilon_d^2 + \Gamma^2/4\right)/2\pi}{\left[E^2 - 2EM(E) - \epsilon_d^2 + \frac{\Gamma^2}{4}\right]^2 + \Gamma^2\{\epsilon_d^2 + [M(E)]^2\}} \ , \\
\rho_2(E) &= \frac{\Gamma\left\{[E - 2M(E)]^2 + \epsilon_d^2 + \Gamma^2/4\right\}/2\pi}{\left[E^2 - 2EM(E) - \epsilon_d^2 + \frac{\Gamma^2}{4}\right]^2 + \Gamma^2\{\epsilon_d^2 + [M(E)]^2\}} \ . \qquad (12)
\end{aligned}
$$

We see that $\rho_i(E)$ with $i = 1, 2$ are even functions of E, i.e. $\rho_i(-E) = \rho_i(E)$, which arises from the fact that γ_i are real fermions. The behaviors of $\rho_i(E)$ with $i = 1, 2$ are shown in Figs. 7 and 8.

For the on-resonance dot, i.e. $\epsilon_d = 0$, we notice that γ_2 does not couple to the chiral Majorana edge states at all. Thus, its LDOS exhibits a Lorentzian form with a peak at zero energy and width determined by Γ, and is independent of the number of vortices in the TSC. On the other hand, due to the coupling to the chiral Majorana edge states, ρ_1 develops several peaks located at the values of eV/Γ which are the real roots of the equation $x = 2M(x)$, and the peak values are universal in the sense that $2\pi\Gamma(\rho_1)_{\max} = 4$. Hence, the peak values of $G(V)/G_0$ (in units of $\Gamma_L\Gamma_R/\Gamma^2$) are nonuniversal, except that $G(0)/G_0 = 2\Gamma_L\Gamma_R/\Gamma^2, 4\Gamma_L\Gamma_R/\Gamma^2$ for odd and even N_v, respectively. Moreover, $G(V)/G_0$ approaches the value $2\Gamma_L\Gamma_R/\Gamma^2$ as $eV/\Gamma \gg 1$ since $\rho_2(E) \to 0$ when $E/\Gamma \gg 1/2$. On the other hand, ρ_1 becomes zero when $1/M(E) = 0$ or $E = E_l$, where $E_l = \frac{2\pi v_M}{L}[l + (N_v + 1)/2]$ with integer l are the quantized energy levels of the chiral Majorana edge modes. This suggests that the coupling to the chiral Majorana edge states will suppress half of the degrees of freedom for the dot electrons for an on-resonance dot. One may view this as "Majorana-fermionization" of half of the degrees of freedom of dot electrons. In summary, on account of the oscillatory behavior of $\rho_1(E)$, which follows from the coupling to the chiral Majorana edge states, $G(V)$ for an on-resonance dot becomes an oscillating function of eV.

For an off-resonance dot, we notice that the suppression in ρ_1 also occurs whenever E matches the quantized

energy levels of the chiral Majorana edge modes. That is, $\rho_1(E) = 0$ for $E = E_l$. This implies the robustness of "Majorana-fermionization" of dot electrons. Moreover, ρ_1 as well as ρ_2 are oscillatory functions of E due to the coupling to the chiral Majorana edge states and $\epsilon_d \neq 0$. In fact, this oscillation is intimately related to the suppression in ρ_1 at $E = E_l$ since it must obey the sum rule:

$$\int_0^{+\infty} dE\rho_1(E) = \frac{1}{2} .$$

This results in the oscillatory behavior of $G(V)$ as varying eV. The peaks in $G(V)$ are located at the values of $eV/(2\Gamma)$ when they are the real roots of the equation $x^2 - 2M(x)x = (\epsilon_d/\Gamma)^2 \pm 1/4$. Thus, $G(V)/G_0$ takes the universal value $2\Gamma_L\Gamma_R/\Gamma^2$ at these peaks.

IV. CONCLUSION

To sum up, we study the electrical transport through a QD side-coupled to a TSC in the spinless regime. We pay attention to the behavior of the conductance G as varying the bias V. We found that G is an oscillatory function of eV similar to the one for a multi-level dot. However, the function $G(V)$ in the present case is distinguished from that for a multi-level dot in three respects. First of all, the former will shift upon adding or removing a vortex in the TSC, while such an effect is not observed for the latter. Next, for an off-resonance dot, the value of the conductance peak in the former case is only half of the one in the unitary limit, whereas for the latter, it will reach a non-universal value depending on the energy levels in the dot as long as $eV/2$ matches one level in the dot. Finally, for an on-resonance dot, the conductance peak in the former case will approach a universal value $G/G_0 = 2\Gamma_L\Gamma_R/\Gamma^2$ at large bias. In general, there is no such a behavior for the latter. We consider these features the signatures of chiral Majorana edge states.

The oscillatory behavior of $G(V)$ can be understood by introducing the Majorana representation of dot electrons. The dot electron is composed of two Majorana fermions. Only one of them is coupled to the chiral Majorana edge states directly. We show that this coupling results in the suppression in the LDOS whenever the energy matches one of the quantized energy levels of the chiral Majorana edge states. This phenomenon is dubbed as Majorana fermionization because only the other Majorana fermion, which is not directly coupled to the chiral Majorana edge states, survives at these energies. It is interesting to explore similar phenomena in other situations.

Finally, we would like to emphasize that the above results are obtained assuming zero temperature and without other possible dissipations. Extension to the finite temperature can start with Eq. (4). Dissipations arising from the environment, however, involve the change of the model. Dissipation effects may suppress the tunneling rate or cause a nontrivial phase diagram such that the results obtained from the tunneling spectroscopy to identify the signature of the chiral Majorana liquid may be dubious. The effects of ohmic dissipations on the tunneling between the normal metallic lead and the end of a 1D TSC has been studied,[28] which shows distinct temperature behaviors for the zero-bias conductance peaks due to the Majorana fermion end mode and other effects. It deserves to include the dissipation effects into our analysis to see how the results we obtained are modified.

Acknowledgments

The author would like to thank Y.-W. Lee and C.S. Wu for enlightening discussions.

* Electronic address: yllee@cc.ncue.edu.tw

[1] N. Read and D. Green, Phys. Rev. B **61**, 10267 (2000).
[2] V. Gurarie, L. Radzihovsky, and A.V. Andreev, Phys. Rev. Lett. **94**, 230403 (2005).
[3] M. Stone and S.B. Chung, Phys. Rev. B **73**, 014505 (2006).
[4] A.Y. Kitaev, Phys.-Usp. **44**, 131 (2001).
[5] D.A. Ivanov, Phys. Rev. Lett. **86**, 268 (2001).
[6] A.Y. Kitaev, Ann. Phys. (N.Y.) **303**, 2 (2003).
[7] C. Nayak, S.H. Simon, A. Stern, M. Freedman, and S. Das Sarma, Rev. Mod. Phys. **80**, 1083 (2008).
[8] R.M. Lutchyn, J.D. Sau, and S. Das Sarma, Phys. Rev. Lett. **105**, 077001 (2010).
[9] Y. Oreg, G. Refael, and F. von Oppen, Phys. Rev. Lett. **105**, 177002 (2010).
[10] V. Mourik, K. Zuo, S.M. Frolov, S.R. Plissard, E.P.A.M. Bakkers, and L.P. Kowenhoven, Science **336**, 1003 (2012).
[11] E.J.H. Lee, X.C. Jiang, M. Houzet, R. Aguado, C.M. Lieber, and S. De Franceschi, Nature Nano. **9**, 79 (2014), which sheds some light on the controversy about the zero-bias anomaly and its relevancy on the signature of Majorana mode.
[12] L. Fu and C.L. Kane, Phys. Rev. Lett. **100**, 096407 (2008).
[13] C.J. Bolech and E. Demler, Phys. Rev. Lett. **98**, 237002 (2007).
[14] J. Nilsson, A.R. Akhmerov, and C.W.J. Beenakker, Phys. Rev. Lett. **101**, 120403 (2008).
[15] K.T. Law, P.A. Lee, and T.K. Ng, Phys. Rev. Lett **103**, 237001 (2009).
[16] L. Fu and C.L. Kane, Phys. Rev. B **79**, 161408(R) (2009).
[17] K.T. Law and P.A. Lee, Phys. Rev. B **84**, 081304(R) (2011).
[18] P.A. Ioselevich and M.V. Feigelḿan, Phys. Rev. Lett. **106**, 077003 (2011).
[19] M. Leijnse and K. Flensberg, Phys. Rev. B **84**, 140501(R) (2011).
[20] D.E. Liu and H.U. Baranger, Phys. Rev. B **84**, 201308(R)

(2011).
[21] E. Vernek, P.H. Penteado, A.C. Seridonio, and J.C. Egues, Phys. Rev. B **89**, 165314 (2014).
[22] Y. Cao, P. Wang, G. Xiong, M. Gong, and X.Q. Li, Phys. Rev. B **86**, 115311 (2012).
[23] L. Ponomarenko, F. Schedin, M.I. Katsnelson, R. Yang, E.W. Hill, K.S. Novoselov, and A.K. Geim, Science **320**, 5874 (2008); J. Güttinger, C. Stampfer, F. Libisch, T. Frey, J. Burgdörfer, T. Ihn, and K. Ensslin, Phys. Rev. Lett. **103**, 046810 (2009).
[24] For a review, see, for example, S. Sapmaz, P. Jarillo-Herrero, L.P. Kouwenhoven, and H.S.J. van der Zant, Semicond. Sci. Technol. **21**, S52 (2006).
[25] J.G. Analytis, R.D. McDonald, S.C. Riggs, J.-H. Chu, G.S. Boebinger, and I.R. Fisher, Nature Phys. **6**, 960 (2010); D.X. Qu, Y.S. Hor, J. Xiong, R.J. Cava, and N.P. Ong, Science **329**, 821 (2010).
[26] Within the context of our setup, the Kondo effect is not significant here. For the discussions on a magnetic impurity coupled to the helical Majorana liquid, i.e. the edge states of the time-reversal invariant TSC, see, for example, R. Žitko and P. Simon, Phys. Rev. B **84**, 195310 (2011). For a discussion on the interplay between the Kondon effect and the Majorana-induced couplings in a QD coupled to the end of a 1D TSC, see, for example, Y. Avishai, Phys. Rev. Lett. **107**, 176802 (2011) and M. Cheng, M. Becker, B. Bauer, and R.M. Lutchyn, arXiv: 1308.4156. See also H. Khim, R. López, J.S. Lim, and M. Lee, arXiv: 1408.5053 for the study on the thermoelectric response of a Konod dot side-coupled to the Majorana fermion at the end of a 1D TSC.
[27] Y. Meir and N.S. Wingreen, Phys. Rev. Lett. **68**, 2512 (1992).
[28] D.E. Liu, Phys. Rev. Lett. **111**, 207003 (2013).